Assessment of Metal Enrichment in the Koma Bangou (Niger) Gold panning Area Soils and Tailings

ABSTRACT

Artisanal and small-scale gold mining at Koma Bangou (Niger) has been going on since the Sahelian 1984's drought, with introduction of ore leaching in the year 2009. The use of chemicals in the ore processing results in metal enrichment and pollution at the cyanidation sites. The aim of this work is to assess the metal enrichment of soils and tailings at Koma Bangou. Geochemical data acquired with portable XRF analyzer corrected with ICP-MS data, were used to assess the enrichment level of As, Cr, Cu, Mn, Pb and Zn in the soils and tailings samples using the enrichment factor and soil-geochemical baseline data for the Koma Bangou soils. The metallic enrichment generated by the ore processing was identified in the tailings (cyanidation and acidification waste) and the soils from the cyanidation areas. The perimeter soils (soils outside cyanidation sites) show no metal enrich-ment. As and Pb enrichment is highest in the cyanidation waste, while Zn, Cu and Cr enrichment is highest in the acidification waste. Mn enrichment is very low in all of the soils and the tailings samples. The gold ore leaching activities generate metallic pollution of the soil, water and vegetation around the cyanidation sites.

Keywords: Koma Bangou, Gold panning, Cyanidation, Tailings, Metal enrichment, Pollution

1. INTRODUCTION

"Artisanal and Small-scale Mining" refers to all artisanal or semi-mechanized mining operations that don't require large equipment and big investment [1-3]. Communities and local economies in many developing countries often depend on revenues generated by this labor-intensive activity [3]. Artisanal gold mining is the main mining sector employer and is carried out in over 80 countries worldwide [4].

Artisanal gold mining began in Niger at the Koma Bangou site in the Tillabéri region [5], following the drought and poor harvests of 1984 in Niger [6-9]. Gold panning is the most widely performed non-agricultural income-generating activity in Niger [6,8]. It was interrupted at Koma Bangou in 1989 due to industrial mining exploration [10]. It was resumed in 1999, with the introduction of hydrometallurgical cyanide ore processing in 2009 [11]. From 1984 to present day, gold panning at Koma Bangou has produced large quantities of tailings [10]. These tailings have a negative impact on the surrounding environment by enriching the soil and water with metals [10-15]. This metallic enrichment may lead to contamination or even metallic pollution of Koma Bangou soil and water [13].

Assessing the metal enrichment in soils is important for the environmental protection. Among geochemical approaches is the enrichment factor (EF). Enrichment factor reflects the degree of metal accumulation [16] and has been widely used in environmental pollution studies [16-20]. It's a universal index for assessing the metal accumulation degree [21]. The enrichment factor reflects also the disturbance degree of the natural environment caused by human activities [22]. Metal concentrations are normalized by a conservative element such as Fe, Al, Ti [17,23] in order to reduce the mineralogical variability and the granulometric variations [24]. The aim of this work is to assess the metal enrichment in soils and tailings of Koma Bangou due to the hydrometallurgical ore processing.

2. MATERIAL AND METHODS

2.1. Study Area

Koma Bangou gold panning area belongs to Téra department, in the Tillabéri region (southwestern part of Niger Republic) [11]. Koma Bangou gold panning area is located between Lat. 14°01'41''N and 14°07'56''N and Long. 01°02'12''E and 01°10'00''E, and covers 150 km^2 [10,12]. Geologically, Koma Bangou is located in the Liptako birimian greenstone belt of Diagorou-Darbani [25] (Fig. 1b). The Liptako Niger forms the northeastern end of the Léo-Man Ridge (Fig. 1a), on the West African craton [26]. Geological features of Koma Bangou (Fig. 1c) consist of metabasalt and metasediment [26-28], with quartz diorite, qabbro, rhyolite and andesite intrusion [28]. The rock is overlain by lateritic and eolian deposits [28].

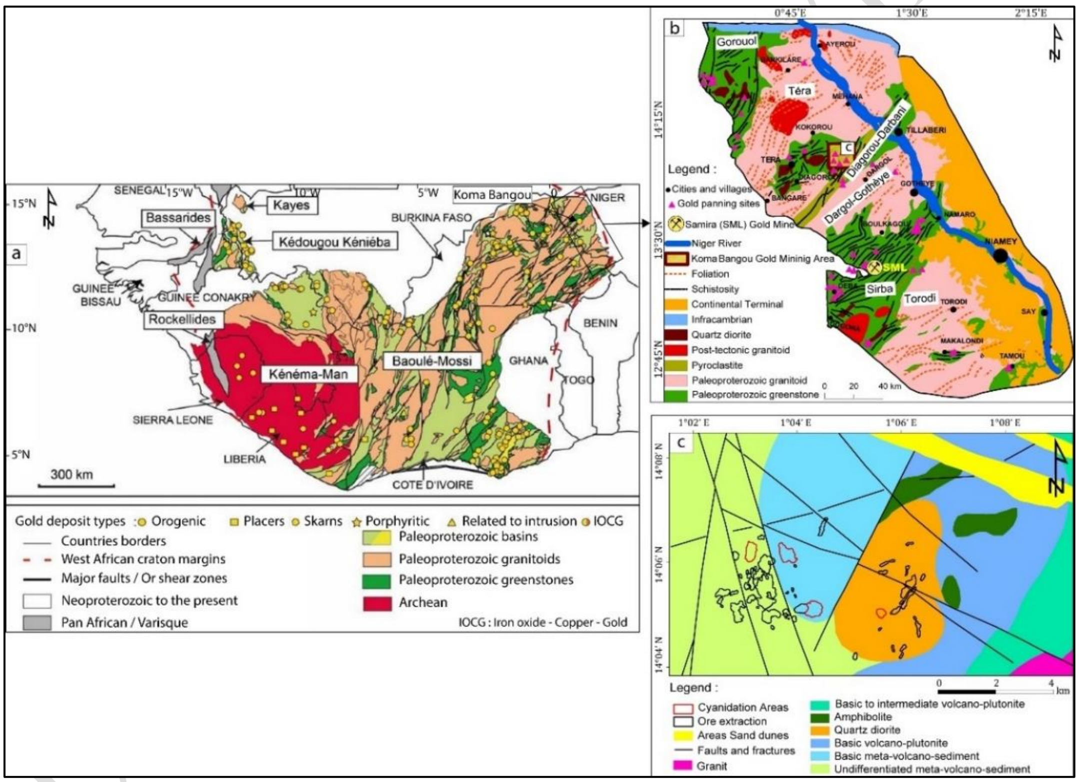

Fig. 1. Geological map of the Léo-Man ridge [31] and location of gold deposits [32]; b) Geological map of Liptako Niger [33]; c) Geological features of Koma Bangou [27].

The Liptako gold mineralization is hosted by greenstone belts and linked to regional faults [29]. The gold mineralization of Koma Bangou is a quartz-vein type, controlled by fractures [28-30]. Sulfides related to the mineralization consist of pyrite, chalcopyrite, chalcocite, sphalerite and galena [10].

Gold ore extraction at Koma Bangou is manual [7]. It involves digging vertical shafts (Fig. 2a) with 0.8 to 2 m in diameter [34] to extract barren rock and mineralized quartz. Shaft sinking is done by hand, using makeshift tools such as pickaxes, picks, hammers, shovels, plastic bags, ropes and flashlights [7]. A manual rope winch (Fig. 2a) is fixed above the hole on wooden supports to raise and lower the workers into the hole, as well as to raise the bags filled with ore or waste rock. Waste rock and ore are brought to the surface. The ore is then sorted and the mineralized quartz undergo to crushing (Fig. 2b), grinding, physical treatment with sluice (Fig. 2c) and chemical cyanide treatment (Fig. 2d) to recover the gold. The gold contained in the cyanide juice is recovered by zinc plates using the Merill-Crowe process [35]. The zinc plates loaded with gold are dissolved with sulfuric and nitric acids to obtain residues containing gold. These residues are then burned with water and sulfuric and nitric acids to obtain the concentrated gold [36].

Fig. 2. Stages of artisanal gold mining at Koma Bangou. a) Ore extraction shaft fitted with winch; b) Manual crushing of ore; c) Gravity concentration of gold in sluice; d) Cyanide leach tanks for gold-bearing ore; e) Spreading of cyanidation waste; f) Acidification waste dump.

2.2. Sampling

Soils (perimeter soils, cyanidation area soils) and tailings (acidification waste and cyanidation waste) samples were collected from Koma Bangou area. Tailings from the ore leaching consist of cyanidation and acidification waste. Cyanidation waste is made up of fine particles of crushed ore that have first undergone to gravity sluicing and then cyanide leaching (Fig. 2e). Acidification waste result from the final stage in the ore leaching chain, which involves acidification of the gold-bearing zinc plates (Fig. 2f). Cyanidation area soils are the soils of the sites where ore leaching operations are carried out. Perimeter soils are soils located outside the sites of the chemical ore processing. Systematic grid sampling for soils and stratified random sampling for tailings were used (Fig. 3). Soil samples were taken with a hand auger at 0-40 cm depth. Tailings samples were taken from the waste piles with shovel. 400 samples: perimeter soils (70), cyanidation area soils (122), acidification waste (27), cyanidation waste (181) were collected.

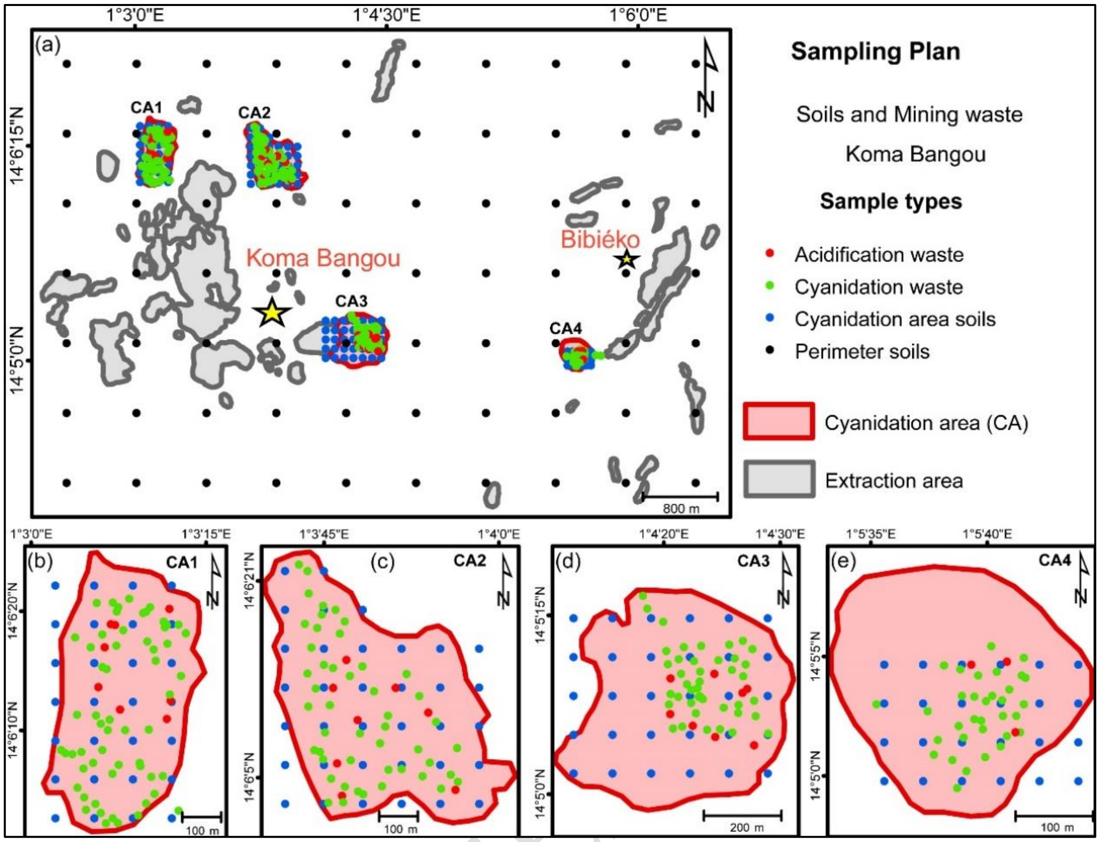

Fig. 3. Sampling plans on the Koma Bangou gold panning area. a) Sampling ground-plan; b, c, d, e) Systematic and stratified random sampling plan on the cyanidation areas.

2.3. Chemical analysis

The 400 samples of soils and tailings were first air-dried, then sieved. The < 2 mm fraction was ground to 75 µm before being analyzed by portable X-ray fluorescence spectrometer (pXRF). XRF analysis was carried out under laboratory conditions at the "UFR STRM" of Félix Houphouët Boigny University, Cocody-Abidjan (Côte d'Ivoire), using a Thermo Niton XL3t XRF analyzer. 55 samples representative of the soils and the tailings were analyzed by inductively coupled plasma mass spectrometry (ICP-MS) at the "CETA-ISO platform, OSU OREME of the University of Montpellier". Soil and tailings samples were first digested with hydrochloric acid (HCl), hydrofluoric acid (HF) and nitric acid (HNO_3). Digested solutions were analyzed using ICP-MS (iCAP TQ, Thermo Scientific®) after dilution in 0.15 M HNO_3. The concentrations of Al, As, Cr, Cu, Fe, Mn, Pb, Ti and Zn were determined using external calibration and correction of the internal standards (Sc, Ge, Rh and Ir) to adjust for variations in sensitivity induced by matrix effect or instrumental drift.

2.4. XRF data correction

XRF data were calibrated with ICP-MS data. XRF data were corrected by using the regression coefficients (Eq. 1).

$$[X]_{ICP\text{-}MS} = \exp(b \pm db)\left([X]_{pXRF}\right)^{(b \pm db)} \quad (1)$$

where:

$[X]_{ICP\text{-}MS}$ is the X element ICP-MS concentration;

$[X]_{pXRF}$ is the X element pXRF concentration;

a, b; da, db are the coefficients of the regression line and their related errors.

2.5. Enrichment assessment

Metal enrichment is assessed using the normalized enrichment factor. The normalized enrichment factor is calculated as the ratio of the element concentration in the normalized sample to a reference concentration [17-19]. The normalization is performed with element that isn't expected to be enriched by anthropogenic sources due to its high natural concentration [37].

The Kolmogorov-Smirnov test [38] was applied to Fe, Al and Ti concentrations to check their distribution in the Koma Bangou perimeter soils. The Kolmogorov-Smirnov test is applied if the number of samples is greater than 50 [39]. The null hypothesis is that the variables are normally distributed [40]. If the p-value is below the 5% alpha (significance level) [38], the null hypothesis is rejected [38]. In this case, the variables don't follow a normal distribution. If the p-value is above alpha, the null hypothesis is accepted [38]. In this case, the variables follow a normal distribution.

Pedo-geochemical baseline values of Al (63095, 73 mg/kg), As (58.05 mg/kg), Cr (172.89 mg/kg), Cu (76.25 mg/kg), Fe (92708.84 mg/kg), Mn (1478.31 mg/kg), Pb (18.95 mg/kg), Ti (3695.41 mg/kg) and Zn (133.29 mg/Kg) in the Koma Bangou perimeter soils [10], obtained by the cumulative frequency distribution curve method [41,42] were used to calculate the elements enrichment factor (Eq. 2) [18,19].

$$\mathrm{EF} = \frac{\left[\frac{\mathrm{Cx}}{\mathrm{Cref}}\right]\mathrm{S}}{\left[\frac{\mathrm{Bx}}{\mathrm{Bref}}\right]\mathrm{B}} \qquad (2)$$

where:

$\left[\frac{\mathrm{Cx}}{\mathrm{Cref}}\right]$S is the ratio of the concentration of the target metal and the reference metal in the sample;

$\left[\frac{\mathrm{Bx}}{\mathrm{Bref}}\right]$B is the ratio of the concentration of the target metal and the reference metal in the background material.

The following metal enrichment categories are recognized: insignificant enrichment from natural source (EF < 1) and anthropogenic enrichment (EF ≥ 1) [23]: minor enrichment (1 ≤ EF < 2), moderate enrichment (2 ≤ EF < 5), significant enrichment (5 ≤ EF < 20), very high enrichment (20 ≤ EF < 40), and extremely high enrichment (EF ≥ 40) [18–20,23].

To better classify and interpret the metal enrichment values, the logarithm 10 of EF values was used.

3. RESULTS AND DISCUSSION

3.1. Metal enrichment factor

Table 1 gives the statistical values and the normality test result for Fe, Al and Ti in the Koma Bangou perimeter soils. Only Ti follows a normal distribution and was chosen as the enrichment factor normalizer for the As, Cr, Cu, Mn, Pb and Zn.

Table 1. Statistics values and Kolmogorov-Smirnov test results for Fe, Al and Ti.

Element	Descriptive statistics				Normality test	
	TN	Min	Mean	Max	p-value	Decision (5% significance)
Al	70	6154	21902	71556	0	Rejected
Fe	70	22211	60503	224789	0.01	Rejected
Ti	70	398	2417	5441	0.15	Accepted

TN: Total Number; Min: Minimum; Max: maximum

Table 2 gives the enrichment factor (EF) statistical values for As, Cr, Cu, Mn, Pb and Zn in the Koma Bangou soils and tailings samples.

Table 2. EF Statistical values for As, Cr, Cu, Mn, Pb and Zn.

EF	Sample types	TN	Min	Mean	Max
As EF	Cyanidation area soils	122	0.37	17.75	140.04
	Cyanidation waste	181	0.32	34.96	758.14
	Acidification waste	27	1.61	24.05	183.04
	Perimeter soils	70	0.08	1.40	9.36
Cr EF	Cyanidation area soils	122	0.34	1.12	2.89
	Cyanidation waste	181	0.28	1.30	2.74
	Acidification waste	27	2.58	5.22	13.20
	Perimeter soils	70	0.34	1.18	5.41
Cu EF	Cyanidation area soils	122	0.73	3.10	11.33
	Cyanidation waste	181	0.62	5.98	37.21
	Acidification waste	27	3.48	29.46	157.48
	Perimeter soils	70	0.69	1.78	7.43
Mn EF	Cyanidation area soils	122	0.15	0.77	3.15
	Cyanidation waste	181	0.39	1.00	3.33
	Acidification waste	27	0.16	0.96	5.36
	Perimeter soils	70	0.18	0.70	7.07
Pb EF	Cyanidation area soils	122	0.77	23.01	217.97
	Cyanidation waste	181	0.45	44.96	490.63
	Acidification waste	27	5.77	38.81	121.81
	Perimeter soils	70	0.11	1.21	6.56
EF Zn	Cyanidation area soils	122	0.06	14.45	191.48
	Cyanidation waste	181	0.26	15.32	169.81
	Acidification waste	27	79.96	793.35	5943.62
	Perimeter soils	70	0.04	0.80	18.51

According to the average values of As EF (Table 2), cyanidation waste (As EF = 34.96) and acidification waste (As EF = 24.05) have very high enrichment; cyanidation areas soils (As EF = 17.75) have significant enrichment, while perimeter soils (As EF = 1.40) have minor enrichment. According to EF classification (Fig. 4), As enrichment is higher in the cyanidation waste. 178 samples out of 181 (98.34%) of the cyanidation waste show minor to extremely high enrichment (Fig. 4). Only 3 samples from CA1 show insignificant enrichment. All acidification waste samples show minor to extremely high enrichment (Fig. 4). 117 of 122 samples (95.90%) from the cyanidation area soils show minor to extremely high enrichment (Fig. 4). Only 5 samples (2 from CA1, 1 from CA2 and 2 from CA3) show insignificant enrichment. 44 samples out of 70 (62.86%) of the perimeter soils showed insignificant enrichment (Fig. 4).

According to the average values of Cr EF (Table 2), acidification waste (EF Cr = 5.22) has significant enrichment; cyanidation waste (EF Cr = 1.30), cyanidation area soils (EF Cr = 1.12) and perimeter soils (EF Cr = 1.18) have minor enrichment. Depending on the EF classification (Fig. 5), Cr enrichment is higher in the acidification waste. All acidification waste samples show moderate to significant enrichment (Fig. 5).

Cyanidation waste, cyanidation area soils and perimeter soils samples show insignificant to moderate enrichment (Fig. 5).

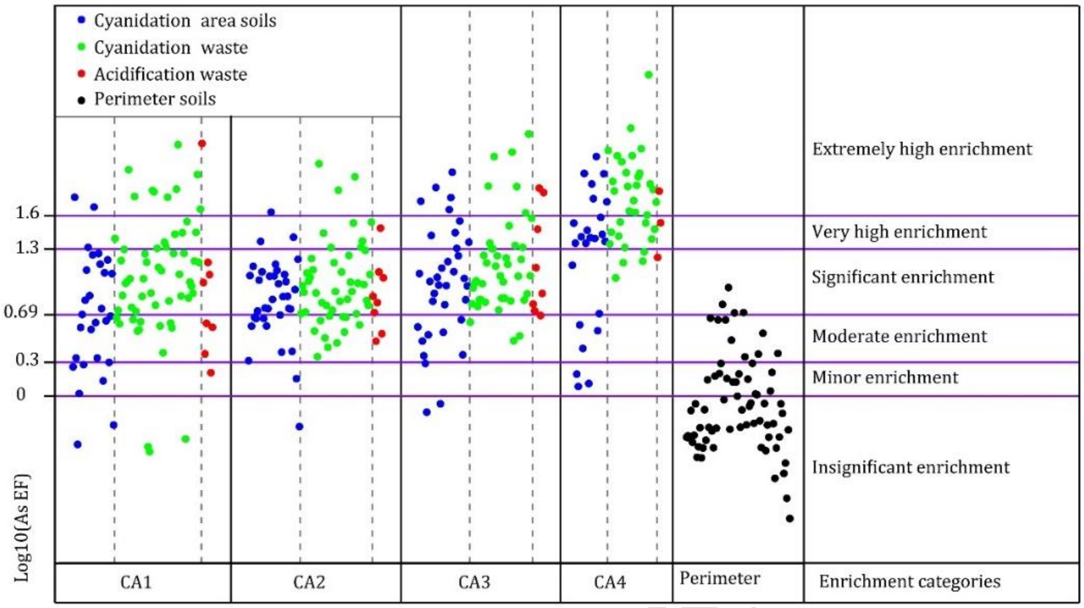

Fig. 4. Classification of the As EF in the Koma Bangou ASGM area samples.

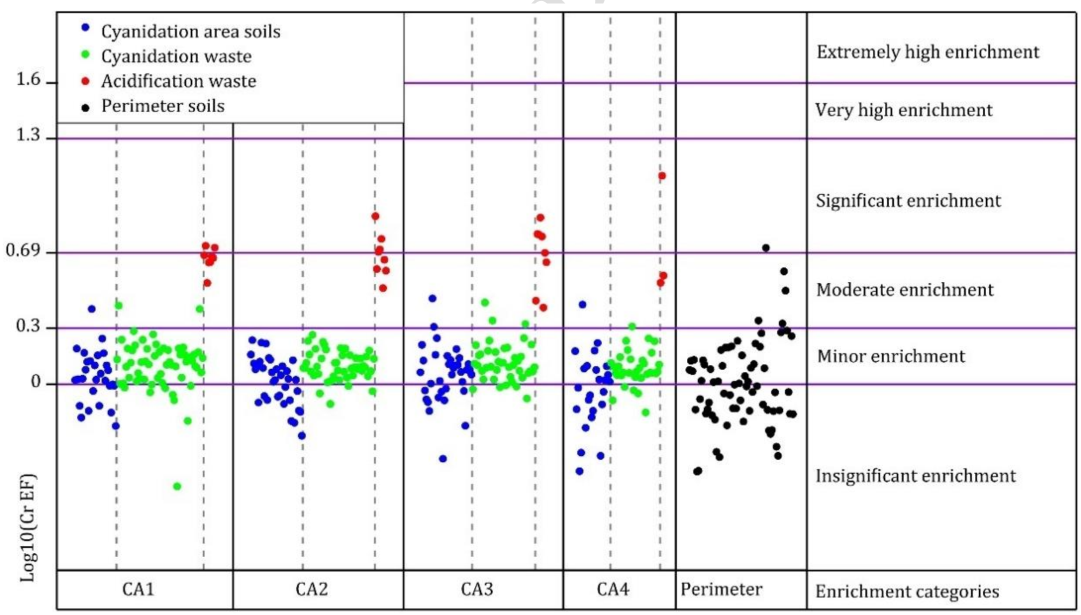

Fig. 5. Classification of the Cr EF in the Koma Bangou ASGM area samples.

According to the average values of Cu EF (Table 2), acidification waste (EF Cu = 29.46) shows very high enrichment; cyanidation waste (EF Cu = 5.98) shows significant enrichment; cyanidation area soils (EF Cu = 3.10) show moderate enrichment and perimeter soils (EF Cu = 1.78) show minor enrichment. According to the EF classification (Fig. 6), Cu enrichment is highest in the acidification waste. All acidification waste samples show moderate to extremely high enrichment (Fig. 6). 178 out of 181 (98.34%) of the cyanidation waste samples show moderate to very high enrichment. Only 3 samples from CA1 show insignificant enrichment. 112 out of 122 (91.80%) of the cyanidation area soil samples show minor to significant enrichment. Only 10 samples show insignificant enrichment (3 from CA1, 3 from CA2, 1 from CA3 and 3 from CA4). 69 samples out of 70 of the perimeter soil show insignificant to moderate enrichment. Only 1 sample shows significant enrichment (Fig. 6).

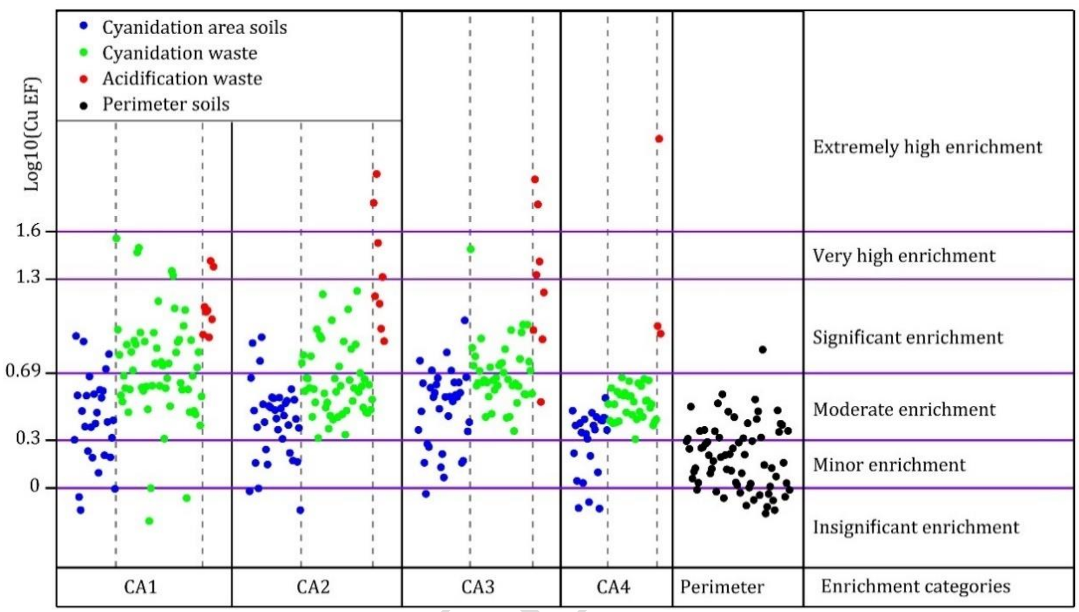

Fig. 6. Classification of the Cu EF in the Koma Bangou ASGM area samples.

According to the average values of Mn EF (Table 2), only cyanidation waste (FE Mn = 1) shows minor enrichment. Acidification waste (FE Mn = 0.96), cyanidation area soils (FE Mn = 0.77) and perimeter soils (FE Mn = 0.70) show insignificant enrichment. Depending on the EF classification, Mn enrichment is low in all the sample types (Fig. 7). Only 5 out of 27 of the acidification waste samples (2 from CA1, 2 from CA3 and 1 from CA4) show minor to significant enrichment (Fig. 7). Only 74 samples out of 181 from the cyanidation waste (27 from CA1, 19 from CA2, 16 from CA3 and 12 from CA4) and 21 samples out of 122 from the cyanidation area soils (11 from CA1, 4 from CA2, 4 from CA3 and 2 from CA4) show minor to moderate enrichment (Fig. 7). Only 7 out of 70 from the perimeter soil samples show minor to significant enrichment (Fig. 7).

According to the average values of Pb EF (Table 2), cyanidation waste (FE Pb = 44.96) has extremely high enrichment; acidification waste (FE Pb = 38.81) and cyanidation area soils (FE Pb = 23.01) have very high enrichment; perimeter soils (FE Pb = 1.21) have minor enrichment. According to the EF classification (Fig. 8), Pb enrichment is higher in the cyanidation waste. 179 out of 181 (98.90%) from the cyanidation waste samples show moderate to extremely high enrichment (Fig. 8). Only 2 samples from CA1 show insignificant enrichment. All the acidification waste samples show significant to extremely high enrichment (Fig. 8). 118 out of 122 (96.72%) from the cyanidation area soil samples show minor to extremely high enrichment (Fig. 8). Only 4 samples (1 from CA1, 1 from CA2, 1 from CA3 and 1 from CA4) show insignificant enrichment. 45 out of 70 (64.29%) from the perimeter soils samples show insignificant enrichment (Fig. 8).

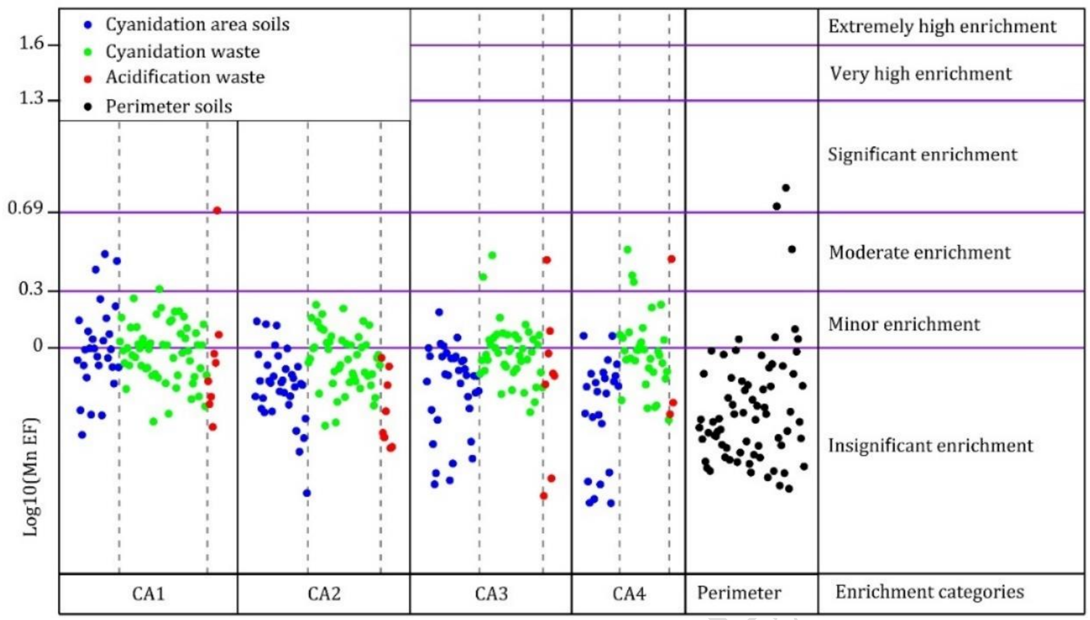

Fig. 7. Classification of the Mn EF in the Koma Bangou ASGM area samples.

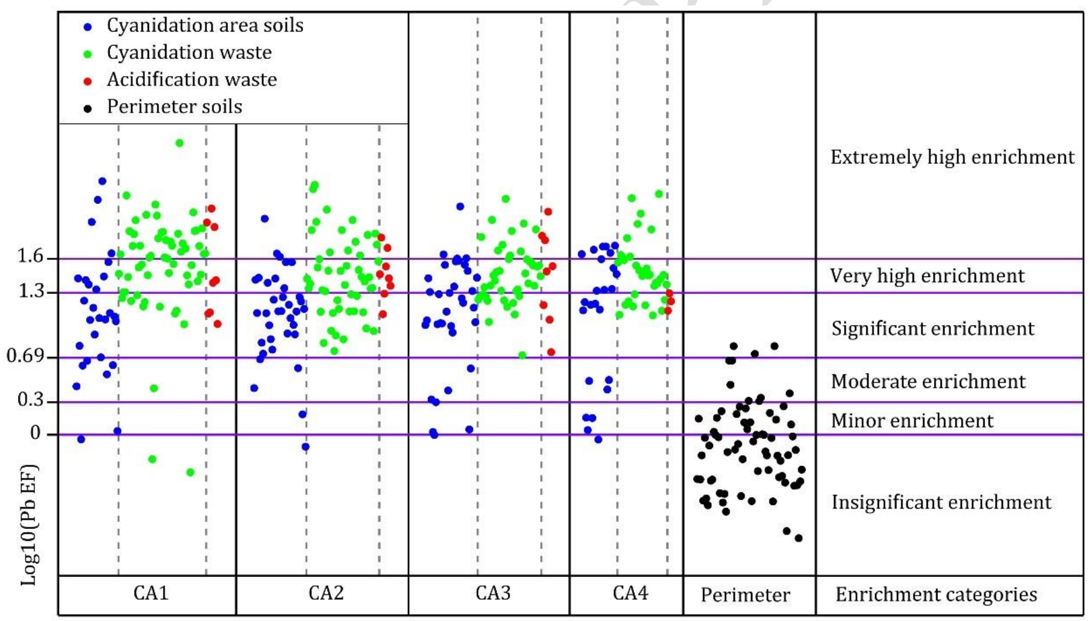

Fig. 8. Classification of the Pb EF in the Koma Bangou ASGM area samples.

According to the average values of Zn EF (Table 2), acidification waste (Zn EF = 793.35) shows very extremely high enrichment; cyanidation waste (Zn EF = 15.32) and cyanidation area soils (Zn EF = 14.45) show significant enrichment, perimeter soils (Zn EF = 0.80) show insignificant enrichment. According to the EF classification (Fig. 9), Zn enrichment is higher in the acidification waste. All the acidification waste samples show very extremely high enrichment (Fig. 9). 179 samples out of 181 (98.90%) of the cyanidation waste show moderate to extremely high enrichment. Only 2 samples (1 from CA1 and 1 from CA3) show insignificant enrichment (Fig. 9). 112 out of 122 (91.80%) of the cyanidation area soil samples show minor to extremely high enrichment. Only 10 cyanidation area soil samples (2 from CA1, 3 from CA3 and 5 from CA4) show insignificant enrichment (Fig. 9). 59 out of 70 form the perimeter soil samples show insignificant enrichment. Only 11 samples (15.71%) show minor to significant enrichment (Fig. 9).

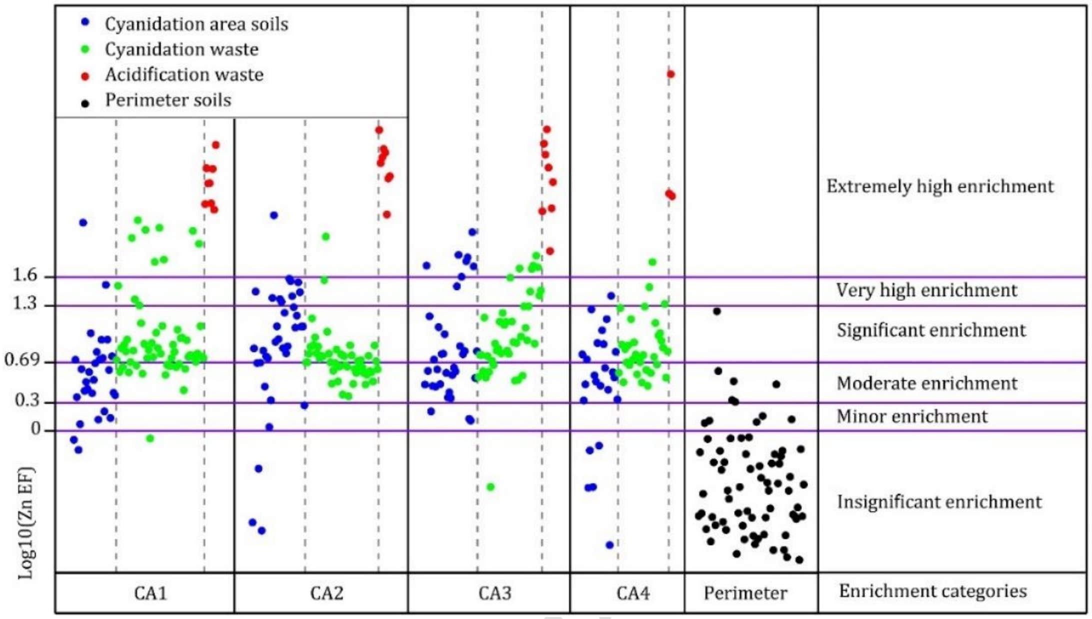

Fig. 9. Classification of the Zn EF in the Koma Bangou ASGM area samples.

3.2. Synthesis of metal enrichment

Fig. 10. shows the enrichment factor values for As, Cr, Cu, Mn, Pb and Zn in the Koma Bangou soils and tailings. The highest enrichment factor values are observed for Zn in the acidification waste, followed by As and Pb in the cyanidation waste, Cu and Cr in the acidification waste and finally Mn in the perimeter soils.

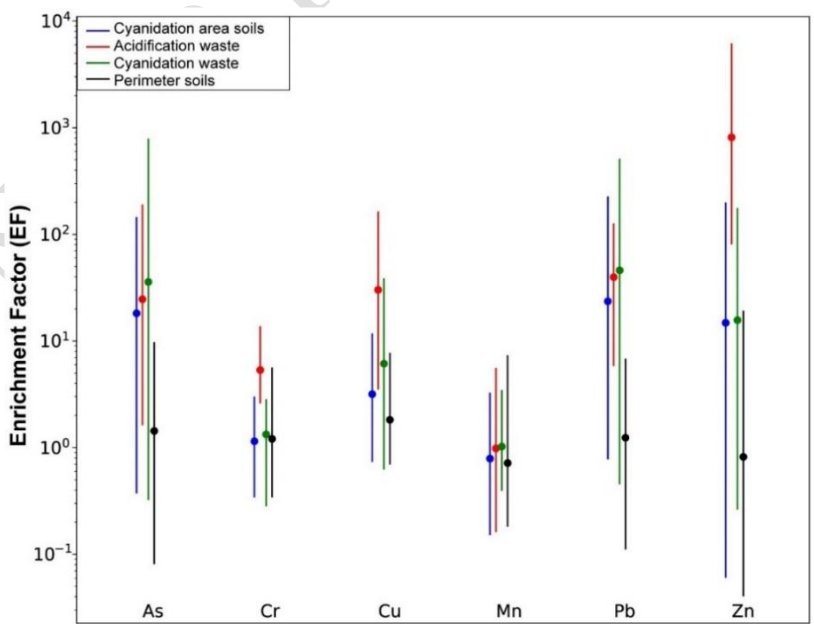

Fig. 10. Synthesis of the elements EF in the Koma Bangou samples.

3.3. Discussion

The results of the enrichment factor show As, Cr, Cu, Pb and Zn enrichment in the samples of acidification waste, cyanidation waste and cyanidation areas soils. As and Pb enrichment was highest in the cyanidation waste. Cr, Cu and Zn enrichment is higher in the acidification waste. Mn enrichment is insignificant in all the sample types, although it is more significant in the perimeter soils. As, Cr, Cu, Pb and Zn enrichment in the acidification and cyanidation waste may occur during the cyanide leaching of the gold-bearing ore, as shown by Abass-Saley [10]. The fact that As and Pb are highly enriched in the cyanidation waste could be explained by the insolubility of As and Pb during the ore leaching. The insolubility of Pb and As in cyanide solution was demonstrated by Goettmann & Hesse [43]. Riveros et al. [44] showed that As occurs as stable (insoluble arsenic iron oxides) under most surface conditions. Goettmann & Hesse [43] have shown that Pb is absorbed by the cyanide solution in the form of a highly stable hydroxo-chloride complex. During the ore leaching with cyanide, certain soluble metals such as Cr, Cu and Zn present in the ore can be brought into solution and precipitate together with gold to form cyanide-metal complexes. The formation of cyanide-metal complexes during gold leaching was demonstrated by Goettmann & Hesse [43]. Metal enrichment is higher in the acidification waste followed by the cyanidation waste and the cyanidation area soils, than in the perimeter soils which are characterized by very low metal enrichment. The metal enrichment around the cyanidation sites is due to the chemical processing of the ore in the sites [10]. The very extremely high enrichment of As, Cr, Cu, Pb and Zn in the acidification and cyanidation waste has led to metal pollution of the soil, water and vegetation around the cyanidation sites. Alassane-Boukari et al. [45], Tankari-Dan-Badjo et al. [13] and Zakaria-Ibrahim et al. [14,15] highlighted the soil, water and vegetation pollution around the cyanidation sites of Koma Bangou.

4. CONCLUSION

Artisanal gold mining at Koma Bangou has led to metal enrichment in the soils and tailings from the cyanidation sites. Data from the soil-geochemical baseline of the Koma Bangou area were used to assess the enrichment level of As, Cr, Cu, Mn, Pb and Zn in the soils and tailings, using the enrichment factor. The latter showed that the enrichment of As, Cr, Cu, Pb and Zn is associated to the cyanidation sites samples (cyanidation area soils, acidification waste, cyanidation waste). As and Pb enrichment is highest in the cyanidation waste, while Zn, Cu and Cr enrichment is highest in the acidification waste. All of the soils and tailings samples show insignificant enrichment of Mn. Metal enrichment at Koma Bangou is essentially anthropogenic, linked to the chemical processing of the gold-bearing ore. It is highest in the acidification waste, followed by the cyanidation waste and the cyanidation area soils. The perimeter soils are unaffected by the ore processing activities and show natural metal enrichment. Metallic enrichment at the Koma Bangou cyanidation sites is mainly due to the use of chemicals in the hydrometallurgical processing and the discharge of tailings into the environment. The chemical processing of gold ore results in metal pollution of soil, water and vegetation around the leaching sites.

REFERENCES

[1] CEA. (1992). Situation de l'exploitation minière à petite échelle en Afrique et stratégie pour son développement. Nations Unies, Rapport Final No. NRD/MRU/TP/I/92, p. 90. https://repository.uneca.org/handle/10855/14990

[2] Hilson, G., Hilson, A., Maconachie, R., McQuilken, J., & Goumandakoye, H. (2017). Artisanal and small-scale mining (ASM) in sub-Saharan Africa: Re-conceptualizing formalization and 'illegal' activity. Geoforum, 83, 80–90. https://doi.org/10.1016/j.geoforum.2017.05.004

[3] USAID. (2017). Sector environmental guideline: artisanal and small-scale mining. Rapport Final No. AID-OAA-M-13-00018, p. 95. https://www.usaid.gov/sites/default/files/2022-05/SectorEnvironmentalGuidelines_Mining_2017.pdf

[4] Hruschka, F. (2022). Une nouvelle tentative de dénombrement des mineurs ASM dans le monde. Retrieved December 24, 2023, from https://www.planetgold.org/fr/renewed-attempt-counting-worlds-asm-miners

[5] Raineri, L. (2020). Gold Mining in the Sahara-Sahel: The Political Geography of State-making and Unmaking. The International Spectator, 55(4), 100–117. https://doi.org/10.1080/03932729.2020.1833475

[6] Hilson, G., Goumandakoye, H., & Diallo, P. (2019). Formalizing artisanal mining 'spaces' in rural sub-Saharan Africa: The case of Niger. Land Use Policy, 80, 259–268. https://doi.org/10.1016/j.landusepol.2018.09.023

[7] Pétot, J. (1995). Réorganisation et modernisation de la petite industrie de l'orpaillage au Liptako (Niger). Projet SI/NER/93/803/11-51 No. 21201, p. 85.

[8] Amadou, A. R. (2002). Propositions pour l'optimisation de la mine artisanale au Niger. Proposals for optimising artisanal mining in Niger. Pangea Infos, Société Géologique de France, 37(38), 18. https://hal-insu.archives-ouvertes.fr/insu-00947881

[9] Yonlihinza, I. A. (2011). Transports et désenclavement dans la problématique du développement local à Téra au Niger. Thèse de Doctorat, Université Toulouse le Mirail - Toulouse II. https://tel.archives-ouvertes.fr/tel-00675205

[10] Abass-Saley, A. (2024). Apport de la télédétection et de la géochimie à l'évaluation de l'impact environnemental de l'exploitation minière artisanale de l'or à Koma Bangou (Liptako, Niger). Thèse de Doctorat, Institut National Polytechnique Houphouët-Boigny, Côte d'Ivoire.

[11] Abass-Saley, A., Baratoux, D., Baratoux, L., Ahoussi, K. E., Yao, K. A., & Kouamé, K. J. (2021). Evolution of the Koma Bangou Gold Panning Site (Niger) From 1984 to 2020 Using Landsat Imagery. Earth and Space Science, 8(11), 25. https://doi.org/10.1029/2021EA001879

[12] Tankari-Dan-Badjo, A, Tidjani, D., Idder, T., Guero, Y., Dan Lamso, N., Matsallabi, A., et al. (2015). Diagnostic de la contamination des eaux par les éléments traces métalliques dans la zone aurifère de Komabangou – Tillabéri, Niger. International Journal of Biological and Chemical Sciences, 8(6), 2849. https://doi.org/10.4314/ijbcs.v8i6.41

[13] Tankari-Dan-Badjo, Abdourahamane, Zakaria-Ibrahim, O., Guéro, Y., Morel, J.-L., Feidt, C., & Echevarria, G. (2019). Impacts of artisanal gold mining on soil, water and plant contamination by trace elements at Komabangou, Western Niger. Journal of Geochemical Exploration, 205(2019), 106328. https://doi.org/10.1016/j.gexplo.2019.06.010

[14] Zakaria-Ibrahim, O., Tankari-Dan-Badjo, A., Elhadj-Daou, I., Abdou-Gado, F., Jean-Marie-Ambouta, K., & Yadji, G. (2018). Impact of gold

mining on vegetation at komabangou area. International Journal of Current Research, 10, 5. https://doi.org/10.24941/ijcr.32761.10.2018

[15] Zakaria-Ibrahim, O., Tankari-Dan-Badjo, A., Guero, Y., Maissoro-Malan-Idi, F., Feidt, C., Sterckeman, T., & Echevarria, G. (2019). Distribution spatiale des éléments traces métalliques dans les sols de la zone aurifère de Komabangou au Niger. International Journal of Biological and Chemical Sciences, 13(1), 557. https://doi.org/10.4314/ijbcs.v13i1.43

[16] Xu, J., Chen, Y., Zheng, L., Liu, B., Liu, J., & Wang, X. (2018). Assessment of Heavy Metal Pollution in the Sediment of the Main Tributaries of Dongting Lake, China. Water, 10(8), 1060. https://doi.org/10.3390/w10081060

[17] Ghrefat, H., Zaman, H., Batayneh, A., El Waheidi, M. M., Qaysi, S., Al-Taani, A., et al. (2021). Assessment of Heavy Metal Contamination in the Soils of the Gulf of Aqaba (Northwestern Saudi Arabia): Integration of Geochemical, Remote Sensing, GIS, and Statistical Data. Journal of Coastal Research, 37(4). https://doi.org/10.2112/JCOASTRES-D-20-00137.1

[18] Gope, M., Masto, R. E., George, J., & Balachandran, S. (2018). Tracing source, distribution and health risk of potentially harmful elements (PHEs) in street dust of Durgapur, India. Ecotoxicology and Environmental Safety, 154, 280–293. https://doi.org/10.1016/j.ecoenv.2018.02.042

[19] Hossain, M. B., Aftad, Md. Y., Yu, J., Choudhury, T. R., Noman, Md. A., Hossain, Md. S., et al. (2022). Contamination and Ecological Risk Assessment of Metal(loid)s in Sediments of Two Major Seaports along Bay of Bengal Coast. Sustainability, 14(19), 12733. https://doi.org/10.3390/su141912733

[20] Tashakor, M., Modabberi, S., van der Ent, A., & Echevarria, G. (2018). Impacts of ultramafic outcrops in Peninsular Malaysia and Sabah on soil and water quality. Environmental Monitoring and Assessment, 190(6), 333. https://doi.org/10.1007/s10661-018-6668-5

[21] Nowrouzi, M., & Pourkhabbaz, A. (2014). Application of geoaccumulation index and enrichment factor for assessing metal contamination in the sediments of Hara Biosphere Reserve, Iran. Chemical Speciation & Bioavailability, 26(2), 99–105. https://doi.org/10.3184/095422914X13951584546986

[22] Harikrishnan, N., Ravisankar, R., Gandhi, Ms., Kanagasabapathy, K., Prasad, M. V. R., & Satapathy, K. (2017). Heavy metal assessment in sediments of east coast of Tamil Nadu using energy dispersive X-ray fluorescence spectroscopy. Radiation Protection and Environment, 40(1), 21. https://doi.org/10.4103/rpe.RPE_67_16

[23] Jahan, S., & Strezov, V. (2018). Comparison of pollution indices for the assessment of heavy metals in the sediments of seaports of NSW, Australia. Marine Pollution Bulletin, 128, 295–306. https://doi.org/10.1016/j.marpolbul.2018.01.036

[24] Hayzoun, H. (2014). Caractérisation et quantification de la charge polluante anthropique et industrielle dans le bassin du Sebou. Thèse de Doctorat, Université Sidi Mohamed ben Abdellah, Fès, Maroc.

[25] Soumaila, A., Garba, Z., Moussa-Issaka, A., Nouhou, H., & Sebag, D. (2016). Highlighting the root of a paleoproterozoic oceanic arc in Liptako, Niger, West Africa. Journal of

Geology and Mining Research, 8(2), 13–27. https://doi.org/10.5897/JGMR2015.0230

[26] Machens, E. (1973). Contribution à l'étude des formations du socle cristallin et de la couverture sédimentaire de l'Ouest de la République du Niger. Mémoires du BRGM No. 82, p. 167.

[27] Abdou, A., Bonnot, H., Bory Kaldey, D., Chalamet, D., Saint Martin, M., & Younfa, I. (1997). Notice explicative des cartes géologiques du Liptako à 1/100000 et 1/200000, p. 64.

[28] Poulin, R., Kima, A., & Savard, R. (1987). Campagne de prospection 1986-87 à Koma Bangou, Niger. Rapport ONAREM, Tome 1 No. 227, p. 209.

[29] Klockner. (1995). Recherche Or dans le Liptako. Direction de la Recherche Géologique et Minière, Projet n° 6500-11-40-026, Rapport Final, p. 162.

[30] Saint-Martin, M. (1999). Projet de prospection minière du Liptako. Direction de la Recherche Géologique et Minière, Rapport Final, p. 457.

[31] Milési, J.-P., Feybesse, J.-L., Pinna, P., Deschamps, Y., Kampunzu, H., Muhonogo, S., et al. (2004). Géologie et principaux gisements de l'Afrique, échelle 1/10,000,000. www.brgm.fr

[32] Markwitz, V., Hein, K. A. A., Jessell, M. W., & Miller, J. (2016). Metallogenic portfolio of the West Africa craton. Ore Geology Reviews, 78, 558–563. https://doi.org/10.1016/j.oregeorev.2015.10.024

[33] Machens, E. (1967). Carte Géologique du Niger occidental. BRGM Orléans.

[34] Ministère de l'Environnement. (2020). Plan d'action national pour l'extraction artisanale et à petite échelle de l'or au Niger, conformément à la convention de Minamata sur le mercure 2021-2025. https://minamataconvention.org/sites/default/files/documents/national_action_plan/Niger-ASGM-NAP-2022-FR.pdf

[35] Oudjehani, K. (2000). Etude du potentiel d'atténuation naturelle des cyanures dans des résidus miniers provenant d'usines de traitement de minerai d'or (Maitrise Génie chimique). Ecole polytechnique de Montréal, Canada.

[36] Zakaria-Ibrahim, O. (2020). Impacts environnementaux et sanitaires des pollutions liées à l'exploitation artisanale de l'or dans la Région de Tillabéry : Cas du site de Komabangou. Thèse de Doctorat, Université Abdou Moumouni.

[37] Costa-Böddeker, S., Hoelzmann, P., Thuyên, L. X., Huy, H. D., Nguyen, H. A., Richter, O., & Schwalb, A. (2017). Ecological risk assessment of a coastal zone in Southern Vietnam: Spatial distribution and content of heavy metals in water and surface sediments of the Thi Vai Estuary and Can Gio Mangrove Forest. Marine Pollution Bulletin, 114(2), 1141–1151. https://doi.org/10.1016/j.marpolbul.2016.10.046

[38] Mishra, P., Pandey, C. M., Singh, U., Gupta, A., Sahu, C., & Keshri, A. (2019). Descriptive Statistics and Normality Tests for Statistical Data. Annals of Cardiac Anaesthesia, 22(1), 67–72. https://doi.org/10.4103/aca.ACA_157_18

[39] Nornadiah, M. R., & Yap, B. W. (2011). Power Comparisons of Shapiro-Wilk, Kolmogorov-Smirnov, Lilliefors and Anderson-Darling Tests. Journal of Statistical Modeling and Analytics, 2(1), 21–33. https://www.nrc.gov/docs/ML1714/ML17143A100.pdf

[40] Şahİntü, L., & Özcan, B. (2017). The comparison of hypothesis tests

determining normality and similarity of samples. Journal of Naval Sciences and Engineering, 13(2), 21–36. https://dergipark.org.tr/tr/download/article-file/402354

[41] Li, X., Yang, Y., Yang, J., Fan, Y., Qian, X., & Li, H. (2021). Rapid diagnosis of heavy metal pollution in lake sediments based on environmental magnetism and machine learning. Journal of Hazardous Materials, 416, 126163. https://doi.org/10.1016/j.jhazmat.2021.126163

[42] Ma, L., Wang, J., & Zhu, L. (2022). Geochemical Baseline of Heavy Metals in Topsoilon Local Scale and Its Application. Polish Journal of Environmental Studies, 31(6), 5805–5813. https://doi.org/10.15244/pjoes/152449

[43] Goettmann, J., & Hesse, A. (2016). Evaluation des données, rapports et expertises d'inventaire existants pour les substances dangereuses stockées dans l'ancien site de stockage souterrain de déchets STOCAMINE, et leur potentiel de mobilisation après le confinement/la fermeture du site minier. K-UTEC AG Salt Technologies, p. 67.

[44] Riveros, P. A., Dutrizac, J. E., & Spencer, P. (2001). Arsenic Disposal Practices in the Metallurgical Industry. Canadian Metallurgical Quarterly, 40(4), 395–420. https://doi.org/10.1179/cmq.2001.40.4.395

[45] Alassane-Boukari, S., Kouassi, E. K. A., Daou, I. E., Soro, Y., & Tankari-Dan-Badjo, A. (2022). Contents of metallic trace elements and pollution parameters in the soils of the Komabangou gold mining area in Niger. J. Mater. Environ. Sci, 13(10), 1227–1241. https://www.jmaterenvironsci.com/Document/vol13/vol13_N10/JMES-2022-13110-Boukari.pdf